



HAL
open science

Atmosphere–soil carbon transfer as a function of soil depth

J. Balesdent, Isabelle Basile-Doelsch, Joel Chadoeuf, Sophie S. Cornu, Delphine Derrien, Zuzana Fekiacova, Christine Hatté

► **To cite this version:**

J. Balesdent, Isabelle Basile-Doelsch, Joel Chadoeuf, Sophie S. Cornu, Delphine Derrien, et al.. Atmosphere–soil carbon transfer as a function of soil depth. *Nature*, 2018, 559 (7715), pp.599-602. 10.1038/s41586-018-0328-3 . hal-02073138

HAL Id: hal-02073138

<https://hal.science/hal-02073138>

Submitted on 21 Mar 2019

HAL is a multi-disciplinary open access archive for the deposit and dissemination of scientific research documents, whether they are published or not. The documents may come from teaching and research institutions in France or abroad, or from public or private research centers.

L'archive ouverte pluridisciplinaire **HAL**, est destinée au dépôt et à la diffusion de documents scientifiques de niveau recherche, publiés ou non, émanant des établissements d'enseignement et de recherche français ou étrangers, des laboratoires publics ou privés.

1 **Atmosphere–soil carbon transfer as a function of soil depth**

2 Jérôme Balesdent^{1*}, Isabelle Basile-Doelsch¹, Joël Chadoeuf², Sophie Cornu¹, Delphine Derrien³, Zuzana
3 Fekiacova¹ & Christine Hatté⁴

4 ¹Aix-Marseille Univ, CNRS, IRD, INRA, Coll France, CEREGE, Aix en Provence, France.

5 ²INRA UR 1052, Avignon, France.

6 ³INRA UR Biogéochimie des Ecosystèmes Forestiers, Nancy, France.

7 ⁴Laboratoire des Sciences du Climat et de l'Environnement, UMR 8212 CEA-CNRS-UVSQ, Université Paris-
8 Saclay, Gif-sur-Yvette, France.

9 *e-mail: jerome.balesdent_a_inra.fr

10
11 **The exchange of carbon between soil organic carbon (SOC) and the atmosphere affects**
12 **the climate^{1,2} and—because of the importance of organic matter to soil fertility—**
13 **agricultural productivity³. The dynamics of topsoil carbon has been relatively well**
14 **quantified⁴, but half of the soil carbon is located in deeper soil layers (below**
15 **30 centimetres)⁵⁻⁷, and many questions remain regarding the exchange of this deep carbon**
16 **with the atmosphere⁸. This knowledge gap restricts soil carbon management policies and**
17 **limits global carbon models^{1,9,10}. Here we quantify the recent incorporation of**
18 **atmosphere-derived carbon atoms into whole-soil profiles, through a meta-analysis of**
19 **changes in stable carbon isotope signatures at 112 grassland, forest and cropland sites,**
20 **across different climatic zones, from 1965 to 2015. We find, in agreement with previous**
21 **work^{5,6}, that the deeper 30–100 centimetres of soil (the subsoil) contains on average 47 per**
22 **cent of the top metre's SOC stocks. However, this subsoil accounts for just 19% of the**
23 **SOC that is newly incorporated (within the past 50 years) into the top metre. Globally,**
24 **the median depth of recent carbon incorporation in mineral soil is 10 centimetres.**
25 **Variations in the relative allocation of carbon to deep soil layers are better explained by**
26 **the aridity index than by mean annual temperature. Land use for crops reduces the**
27 **incorporation of carbon into the soil surface layer, but not into deeper layers. Our results**
28 **suggest that SOC dynamics and its responses to climatic control or land use are strongly**
29 **dependent on soil depth. We propose that using multilayer soil modules in global carbon**
30 **models, tested with our data, could help to improve our understanding of soil–atmosphere**
31 **carbon exchange.**

32 The size of the Earth SOC reservoir is estimated to be around 1,500 gigatonnes of
33 carbon (Gt C) in the first metre, excluding permafrost areas⁶, making it a huge potential source
34 or sink for atmospheric carbon (which increases by +4.4 Gt C per year)¹¹. The future response
35 of this soil compartment could substantially affect not only the climate but also global food
36 production (through the role of organic matter in soil fertility), as well as the stability or
37 resilience of ecosystems³. About half of this carbon is located at depths below 30 cm (refs. ^{5,6}).
38 However, although the dynamics of topsoil carbon has been relatively well quantified,
39 especially thanks to long-term experiments carried out over generations⁴, major questions
40 remain about how to estimate changes in deep-soil carbon and the processes involved.
41 Decision-makers and ecosystem managers are thus deprived of any references for the
42 management of the deep carbon stock. Similarly, when modelling the Earth system and the
43 global carbon cycle, the scientific community also constantly faces the problem of modelling
44 the dynamics of deep carbon^{9,10,12}.

45 Neither absolute changes in carbon stocks nor carbon fluxes in the deep soil horizons
46 can be quantified by direct measurement. Owing to the very low carbon concentrations (on
47 average less than 5 g kg⁻¹ at depths of 80 cm), spatial heterogeneity and slow changes, temporal
48 variations in stocks are smaller than measurement accuracy. Evidence for deep carbon changes
49 is therefore exceptional^{13,14}. Information on incoming fluxes resulting from root mortality and
50 exudation by living roots is not accessible without tracers. In addition, in situ quantification of
51 the outflow from the organic reservoir—which occurs mainly through heterotrophic respiration
52 of the organic matter decomposers, in the form of CO₂ production—is very difficult, if not
53 impossible, because the CO₂ efflux mixes up heterotrophic respiration and root autotrophic
54 respiration¹⁵. Isotopic methods are therefore appropriate for tracing deep carbon dynamics. The
55 radiocarbon age of deep carbon is indicative of its slow turnover¹⁶⁻¹⁹, but ¹⁴C dating, which
56 provides mean ages, does not estimate the exact proportions of active and stable carbon¹⁷⁻²⁰.
57 Here we propose a stable-isotope-based observation of the actual depth distribution of soil
58 carbon ages. It relies on sites that are marked by a natural change in the ¹³C/¹²C ratio of the
59 vegetation at a known date. This is equivalent to the continuous in situ labelling of the
60 atmospheric carbon atoms that have been incorporated into soil organic matter for a known
61 duration, have eventually replaced pre-existing organic carbon, and have been retrieved at the
62 date of sampling²¹.

63 We conducted a meta-analysis of 112 such sites (Extended Data Fig. 1), where the
64 labelling ranged from 4 to 4,000 years. At each site, the technique provides an indication of

65 carbon age—that is, the proportion of carbon that is younger than the labelling duration; meta-
66 analysis of similar sites with varied durations provides an age probability distribution¹⁷. Our
67 study includes most of the world’s biomes except boreal zones, and is evenly distributed among
68 forests, grasslands and croplands.

69 We quantified carbon distribution in the two-dimensional age–depth continuum²², the
70 depth distribution of carbon incorporation in soil over the past 50 years, and the dependence of
71 these factors on climate and land use. We also summarized depth distributions in terms of two
72 layers, 0–30 cm (topsoil) and 30–100 cm (subsoil)—an arbitrary cut-off, but one that is often
73 used in carbon inventories⁶. Our results, which are based on original observations, are
74 independent of any data sets or modelling results from other studies.

75 Figure 1 depicts individual data showing the proportion of new carbon—that is, the
76 proportion of SOC that derives from new vegetation—as a function of time. At all depths, a
77 minor proportion of soil carbon is renewed rapidly (within ten years). Nine sites at which a
78 vegetation signature change occurred more than 1,000 years ago reveal the incomplete
79 replacement of carbon, that is, the presence of millennia-old soil carbon, at depth but not in the
80 topsoil.

81 The rate of carbon incorporation in the topsoil was, as expected, strongly dependent on
82 environmental variables, in particular land use ($P < 0.001$) and mean annual temperature
83 (MAT; $P < 0.05$) (Extended Data Table 1). For the subsoil, by contrast, we found no
84 relationship between carbon age and land use, and only a weak relationship with temperature
85 ($P = 0.1$); instead, carbon age was more affected by the ratio of precipitation to potential
86 evapotranspiration²³ ($P < 0.01$; Extended Data Table 2). This observation reinforces the results
87 of ref. ⁹, which showed that the relationship between ecosystem carbon turnover time and
88 precipitation is pervasive and underestimated by models.

89 To analyse the age distribution with depth under comparable environmental conditions,
90 we selected a homogeneous subset of sites, namely a group of forests and grasslands under
91 warm and moist climates (with MATs higher than 17 °C, annual precipitation of more than
92 1,000 mm, and precipitation/evapotranspiration ratios greater than 0.8). Figure 2 and Extended
93 Data Table 3 depict the detailed depth distribution of carbon ages throughout this panel of soils.
94 This description of carbon dynamics in time–depth space highlights its strong dependence on
95 both variables. The dynamics of subsoil carbon is around seven times slower than that of topsoil
96 carbon (that is, it takes seven times longer to reach the same proportion of renewed carbon;
97 Extended Data Fig. 2). In deep layers, the age distribution reveals the small but non-negligible

98 direct incorporation of photosynthetically fixed carbon through deep roots or soluble carbon
99 (for the youngest carbon), and the predominance of carbon that is older than 1,000 years. Mid-
100 profile horizons (20–70 cm) are dominated by carbon of intermediate ages (100 to 1,000 years),
101 which can be considered to result from the slow downward movement of carbon^{16,24}. Carbon
102 incorporation in the 100–200-cm layer has been quantified in only a few studies and averaged
103 $5 \pm 3\%$ (1 standard deviation) of soil carbon after 50 years.

104 We calculated the amount of carbon incorporated into each layer (C_{new} , in units of
105 kg C m^{-2}) for each site. In our database, the SOC found in the subsoil layer represents 47% of
106 the total stock found in the entire top metre of soil, in agreement with the percentage of 47% to
107 52% reported globally^{5,6}. To express the incorporation of new carbon in depth on the basis of a
108 single indicator, we chose the ratio R_{30-100} , which is $C_{\text{new}}(30-100 \text{ cm})/C_{\text{new}}(0-100 \text{ cm})$, and
109 analysed its dependence on land use, climate and time in the 0- to 200-year-old sites (Extended
110 Data Table 4). We found that R_{30-100} is strongly dependent on land use ($P < 0.001$). The mean
111 values of R_{30-100} (50 years) are 19%, 21% and 29% for forests, grasslands and croplands,
112 respectively. The relatively deeper carbon incorporation in croplands concerns all layers below
113 a depth of 10 cm and cannot be explained only by soil mixing due to ploughing, as the depth of
114 this mixing does not exceed 30 cm (Fig. 3). Croplands incorporate less new carbon in their
115 topsoils than do forests and grasslands, whereas in subsoil the amount of incorporated carbon
116 is similar (Extended Data Tables 1 and 2). This is consistent with the general reduction in
117 carbon input at the soil surface²⁵ that results from the removal of above-ground biomass during
118 harvesting. R_{30-100} also depends on the precipitation/evapotranspiration index ($P < 0.005$), and
119 is weakly dependent on MAT ($P < 0.1$; Extended Data Table 4), in accordance with the deeper
120 rooting that takes place under dry climates, and possibly the more frequent occurrence of deep
121 soils at low latitudes. The world average value of R_{30-100} (50 years) is 19% ($\pm 4\%$; 95%
122 confidence interval) (Fig. 3). The overall shallow incorporation of carbon can be expressed by
123 the median depth of carbon incorporated in the last 50 years: $9 \pm 1 \text{ cm}$ ($\pm 95\%$ confidence
124 interval) in forests, $10 \pm 2 \text{ cm}$ in grasslands and $17.5 \pm 1.5 \text{ cm}$ in croplands in our panel ($9.7 \pm$
125 1.2 cm on average globally; Extended Data Table 5). Taking into account the 100–200-cm layer
126 (when observed) would lower this median depth by 0.5 cm.

127 This study provides an unprecedented estimate of, first, the SOC age distribution over
128 the soil profile (Fig. 2), and, second the depth distribution of the carbon transferred from the
129 atmosphere to soils (Fig. 3). The carbon-incorporation profiles can be compared with existing
130 profiles of root biomass and above-ground inputs. The proportion of carbon that we found to

131 be allocated to the subsoil is higher than the corresponding proportion of root biomass compiled
132 in meta-analyses^{5,26}. This can be explained on the one hand by the contribution of root exudates
133 in addition to root mortality²⁷, and on the other hand by reduced decay rates at depth²⁴. The
134 reduced decay rates could be related to several interacting processes, for example, reduced and
135 scattered microbial biomass⁸, stabilization by minerals^{8,18}, and reduced priming effect (the latter
136 being the stimulation of SOC decomposition by the supply of fresh carbon)²⁸.

137 We measured the depth distribution of atmosphere-derived carbon incorporation over
138 the past 50 years (50-year input). The depth distribution of the net change in soil carbon in the
139 same time interval also depends on the loss of carbon older than 50 years during the period (50-
140 year output). In steady-state systems, the depth distribution of outputs would perfectly equal
141 the depth distribution of inputs. But real systems are transient as a result of global changes in
142 either carbon inputs (for example, increased net primary production, reduced carbon returns
143 because of land-use change) or decay rates (for example, because of warming). On the basis of
144 our meta-analysis, we argue that the depth distributions of carbon output and of carbon
145 incorporation are very similar even in transient systems, for the following reason. In non-
146 steady-state systems, the delay associated with the downward movement of carbon may be
147 suspected to result in 50-year outputs that are deeper than 50-year inputs, in a ‘conveyor-like’
148 dynamic system. But the R_{30-100} ratio increases very slowly with time (by less than 0.001 per
149 year; Extended Data Table 4). This means that the movement of carbon is slow and affects only
150 long-term carbon dynamics, far later than the change expected in future decades. The depth
151 distribution of net changes could differ from our distribution of new carbon only under the
152 pressure of a driving force that affects old carbon in a very different way to the new carbon,
153 such as de-freezing²⁹ or major changes in deep carbon inputs leading to additional priming
154 effects²⁸.

155 Our study also reveals that the steep age gradient with depth (Fig. 2) could be a source
156 of bias in the representation of carbon dynamics if depth is not handled properly. For instance,
157 if we consider three commonly used reference layers—0–10 cm, 0–20 cm and 0–30 cm—we
158 find that their median ages differ considerably, being 23, 50 and 92 years, respectively.
159 Projecting the decay-rate parameters observed in the topmost part of soils onto thicker layers
160 would bias future projections of changes in carbon. The kinetics of carbon incorporation further
161 reveals a substantial turnover over the time range of centuries (Figs. 1, 2 and Extended Data
162 Fig. 2)—that is, between the ‘decadal’ and ‘millennial’ compartments of present carbon

163 models^{1,7,30}—arguing for a more realistic description of carbon storage in terms of continuous
164 time ranges³⁰.

165 Our results show that SOC dynamics and their responses to climatic control or land use
166 are strongly depth dependent. A better representation of deep carbon dynamics has been called
167 for, together with other processes, to improve ecosystem carbon models^{7,12,19}. Our observations
168 support the use of multilayer SOC modules in Earth system models, which our data could help
169 to test.

170 **Online content** Any Methods, including any statements of data availability and Nature Research reporting
171 summaries, along with any additional references and Source Data files, are available in the online version of the
172 paper

173 Received 12 September 2017; accepted 4 May 2018.

- 174 1. Ahlström, A., Schurgers, G., Arneeth, A. & Smith, B. Robustness and uncertainty in terrestrial ecosystem
175 carbon response to CMIP5 climate change projections. *Environ. Res. Lett.* 7, 044008 (2012).
- 176 2. Heimann, M. & Reichstein, M. Terrestrial ecosystem carbon dynamics and climate feedbacks. *Nature* 451,
177 289–292 (2008).
- 178 3. Tiessen, H., Cuevas, E. & Chacon, P. The role of soil organic matter in sustaining soil fertility. *Nature* 371,
179 783–785 (1994).
- 180 4. Rasmussen, P. E. et al. Long-term agroecosystem experiments: assessing agricultural sustainability and
181 global change. *Science* 282, 893–896 (1998).
- 182 5. Jobbágy, E. G. & Jackson, R. B. The vertical distribution of soil organic carbon and its relation to climate
183 and vegetation. *Ecol. Appl.* 10, 423–436 (2000).
- 184 6. Hiederer, R. & Köchy, M. Global Soil Organic Carbon Estimates and the Harmonized World Soil Database
185 (Public. Office EU, 2011).
- 186 7. Todd-Brown, K. E. O. et al. Causes of variation in soil carbon simulations from CMIP5 Earth system models
187 and comparison with observations. *Biogeosciences* 10, 1717–1736 (2013).
- 188 8. Rumpel, C. & Kögel-Knabner, I. Deep soil organic matter—a key but poorly understood component of
189 terrestrial C cycle. *Plant Soil* 338, 143–158 (2011).
- 190 9. Carvalhais, N. et al. Global covariation of carbon turnover times with climate in terrestrial ecosystems. *Nature*
191 514, 213–217 (2014).
- 192 10. Tian, H. Q. et al. Global patterns and controls of soil organic carbon dynamics as simulated by multiple
193 terrestrial biosphere models: current status and future directions. *Glob. Biogeochem. Cycles* 29, 775–792
194 (2015).
- 195 11. Le Quééré, C. et al. Global carbon budget 2016. *Earth Syst. Sci. Data* 8, 605–649 (2016).

- 196 12. Luo, Y. et al. Toward more realistic projections of soil carbon dynamics by Earth system models. *Glob.*
197 *Biogeochem. Cycles* 30, 40–56 (2016).
- 198 13. Guan, X. K. et al. Soil carbon sequestration by three perennial legume pastures is greater in deeper soil layers
199 than in the surface soil. *Biogeosciences* 13, 527–534 (2016).
- 200 14. Hobbey, E., Baldock, J., Hua, Q. & Wilson, B. Land-use contrasts reveal instability of subsoil organic carbon.
201 *Glob. Change Biol.* 23, 955–965 (2017).
- 202 15. Chen, G., Yang, Y. & Robinson, D. Allometric constraints on, and trade-offs in, belowground carbon
203 allocation and their control of soil respiration across global forest ecosystems. *Glob. Change Biol.* 20, 1674–
204 1684 (2014).
- 205 16. Elzein, A. & Balesdent, J. Mechanistic simulation of vertical distribution of carbon concentrations and
206 residence times in soils. *Soil Sci. Soc. Am. J.* 59, 1328–1335 (1995).
- 207 17. Sierra, C. A., Müller, M., Metzler, H., Manzoni, S. & Trumbore, S. E. The muddle of ages, turnover, transit,
208 and residence times in the carbon cycle. *Glob. Change Biol.* 23, 1763–1773 (2017).
- 209 18. Mathieu, J., Hatté, C., Balesdent, J. & Parent, E. Deep soil carbon dynamics are driven more by soil type
210 than by climate: a worldwide meta-analysis of radiocarbon profiles. *Glob. Change Biol.* 21, 4278–4292
211 (2015).
- 212 19. He, Y. et al. Radiocarbon constraints imply reduced carbon uptake by soils during the 21st century. *Science*
213 353, 1419–1424 (2016).
- 214 20. Ahrens, B. et al. Bayesian calibration of a soil organic carbon model using $\Delta^{14}\text{C}$ measurements of soil
215 organic carbon and heterotrophic respiration as joint constraints. *Biogeosciences* 11, 2147–2168 (2014).
- 216 21. Balesdent, J. & Mariotti, A. in *Mass Spectrometry of Soils* (eds Boutton, T. W. & Yamasaki, S. I.) 83–111
217 (Marcel Dekker, New York, 1996)
- 218 22. Lehmann, J. & Kleber, M. The contentious nature of soil organic matter. *Nature* 528, 60–68 (2015).
- 219 23. Trabucco, A. & Zomer, R. Global Aridity Index (Global-Aridity) and Global Potential Evapo-Transpiration
220 (Global-PET) Geospatial Database (CGIAR, Consortium for Spatial Information, 2009).
- 221 24. Guenet, B. et al. The relative importance of decomposition and transport mechanisms in accounting for soil
222 organic carbon profiles. *Biogeosciences* 10, 2379–2392 (2013).
- 223 25. Guo, L. & Gifford, R. Soil carbon stocks and land use change: a meta-analysis. *Glob. Change Biol.* 8, 345–
224 360 (2002).
- 225 26. Schenk, H. J. & Jackson, R. B. The global biogeography of roots. *Ecol. Monogr.* 72, 311–328 (2002).
- 226 27. Strand, A. E., Pritchard, S. G., McCormack, M. L., Davis, M. A. & Oren, R. Irreconcilable differences: fine-
227 root life spans and soil carbon persistence. *Science* 319, 456–458 (2008).
- 228 28. Fontaine, S. et al. Stability of organic carbon in deep soil layers controlled by fresh carbon supply. *Nature*
229 450, 277–280 (2007).

230 29. Koven, C. D. et al. Permafrost carbon-climate feedbacks accelerate global warming. Proc. Natl Acad. Sci.
231 USA 108, 14769–14774 (2011).

232 30. Manzoni, S., Katul, G. G. & Porporato, A. Analysis of soil carbon transit times and age distributions using
233 network theories. J. Geophys. Res. 114, G04025 (2009).

234 **Acknowledgements** We thank C. Marol, S. Milin and P. Signoret for contributing to additional isotopic analyses,
235 as well as the scientists who provided numerical data from their published studies. We thank the French Agence
236 Nationale de la Recherche for funding through the projects Deducas (14-CE01-0004) and Equipex Aster-CEREGE
237 (ANR-10-EQPX-24) and for supporting the Institute National de la Recherche Agronomique (INRA) Laboratory
238 UR-1138 through the Laboratory of Excellence ARBRE (ANR-11-LABX-0002-01). This is a LSCE contribution
239 # 6464.

240 **Author contributions** J.B. led the study and drafted the manuscript. All authors contributed equally to data
241 provision and processing, and commented on and provided edits to the original manuscript. J.C. supervised the
242 statistical analysis.

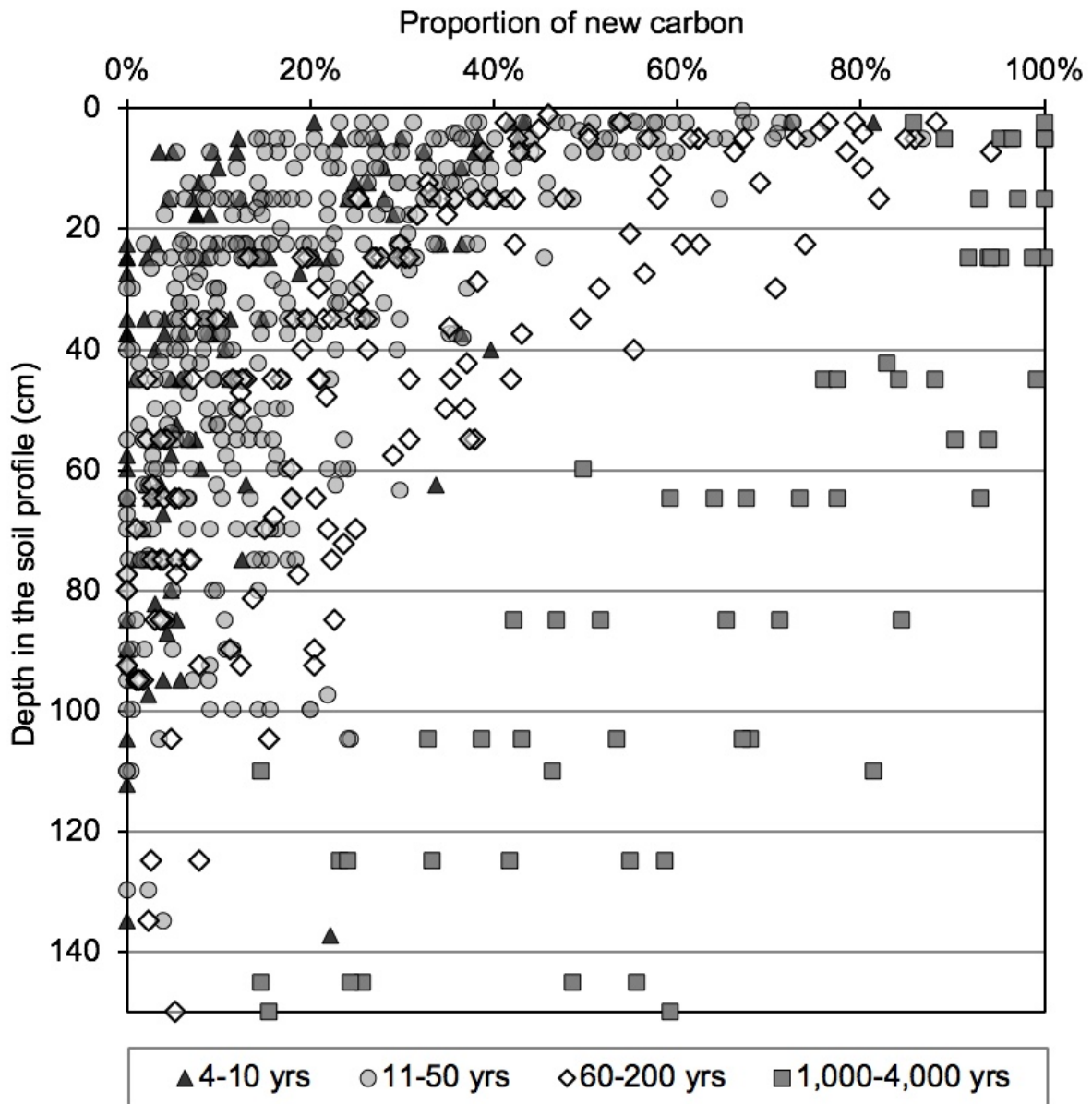
243 **Competing interests** The authors declare no financial competing interests.

244 **Extended data** is available for this paper

245 **Supplementary information** is available for this paper

246 **Correspondence and requests for materials** should be addressed to J.B.

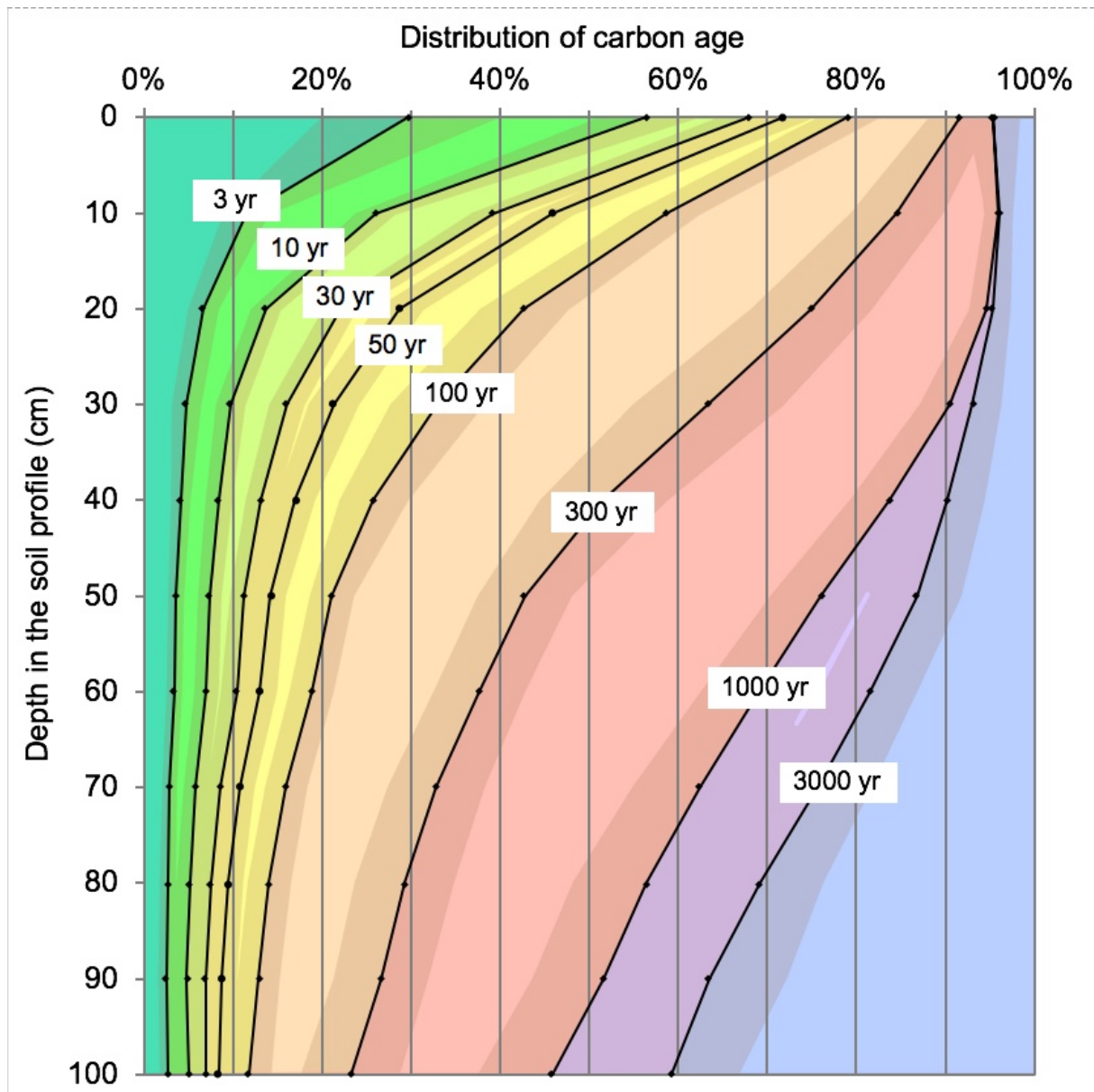
247



248

249 **Fig. 1 | Observed proportions of new carbon in 112 soil profiles.** In each soil sample, the
 250 proportion p of new carbon atoms was determined by the change in the soil carbon ^{13}C signature
 251 following a change in the ^{13}C signature of the vegetation for a given duration t ; p is the
 252 proportion of carbon younger than t ²¹. Data are presented in four classes of duration t .

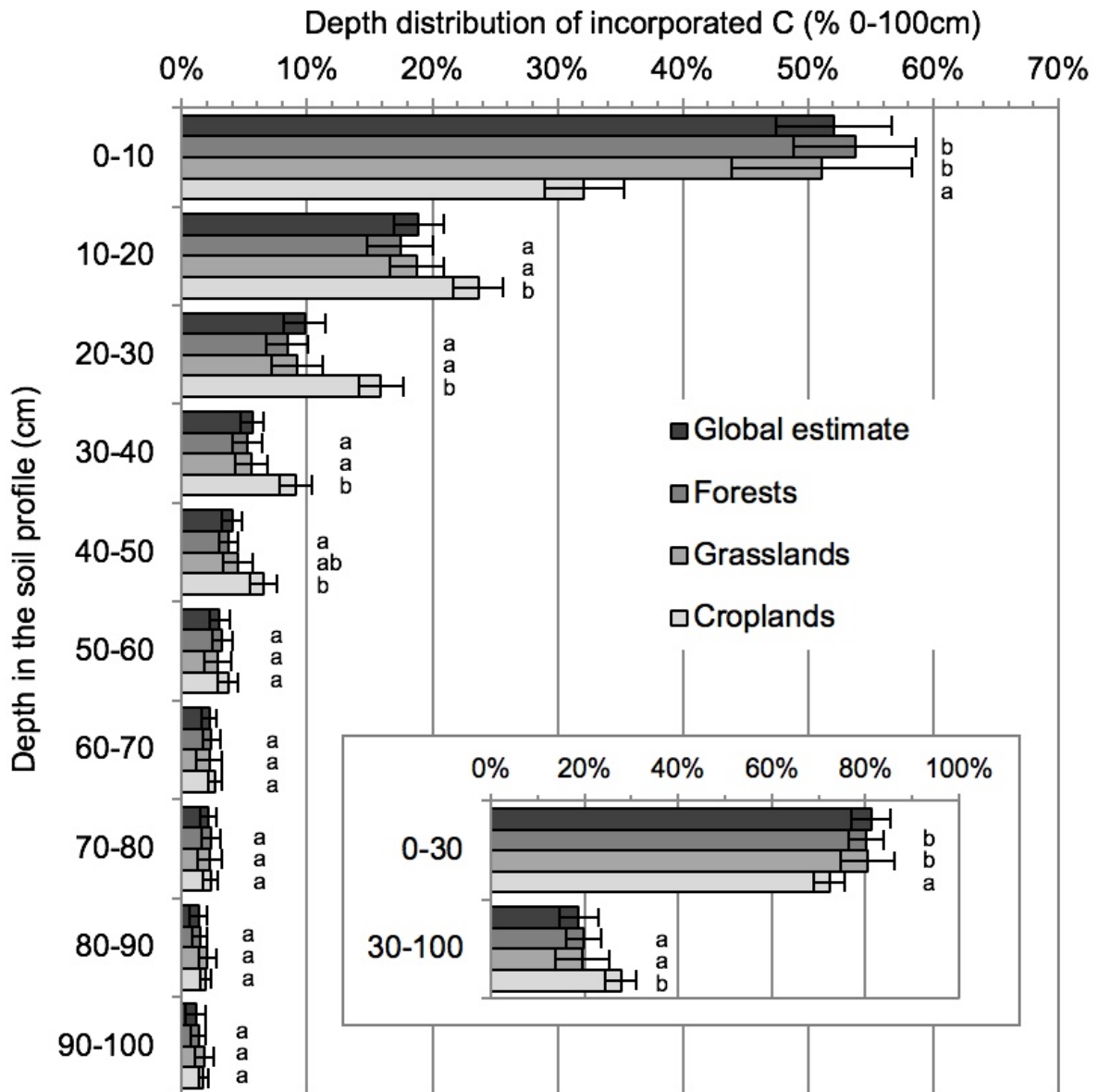
253



254

255 **Fig. 2 | Meta-analysis of carbon age distribution over 55 tropical grassland and forest soil**
 256 **profiles.** At each depth, the proportion of carbon aged less than time t (3 years, 10 years and so
 257 on) was fitted by a bi-exponential regression of t (Extended Data Table 3). Grey bands represent
 258 ± 1 standard error of the estimated mean. The median age of soil carbon increases from seven
 259 years at depth 0 cm to 1,250 years at 100 cm. Integration of the carbon content in each layer
 260 demonstrates that the carbon of age less than 50 years represents 45% of topsoil carbon (0–
 261 30 cm) and 13% of deep carbon (30–100 cm).

262



263

264 **Fig. 3 | Depth distribution of the carbon that has been transferred from the atmosphere**
 265 **to soil organic matter between 1965 and 2015.** The amount of carbon per 10-cm increment
 266 is expressed as a proportion of the total carbon incorporated in the top metre. The value for each
 267 land use is the mean of the observed profiles, and the value for the whole Earth was estimated
 268 by multivariate linear model extrapolation to the world's biomes. Error bars represent the 95%
 269 confidence interval of the mean or estimate; within each increment, land uses followed by the
 270 same letter (a or b) do not differ significantly. The small shift between the global estimate and
 271 the observed values reflects the differences in soil-climate conditions between the global
 272 average and the observation panel.

273

274 **METHODS**

275 **Study sites**

276 We compiled published data sets from 47 peer-reviewed articles, together with original data,
277 on mineral soil $^{13}\text{C}/^{12}\text{C}$ changes in places where the $^{13}\text{C}/^{12}\text{C}$ ratio of the vegetation has been
278 shifted for known durations (see Supplementary Information). We analysed a total of 112 pairs
279 of mineral soil profiles: 108 pairs in which the predominant vegetation has changed from the
280 C3 photosynthetic type to the C4 type, or vice versa, and four pairs from free-air carbon-
281 enrichment (FACE) experiments, where the ^{13}C signature of added carbon dioxide has labelled
282 plant-derived material (Extended Data Fig. 1; see references in Supplementary Information. At
283 each site, two plots with a common history (one with changed and one with unchanged
284 vegetation) were analysed. The isotopic difference between the two profiles was used to
285 calculate the proportion of new carbon through an isotope-mixing equation, which is not biased
286 by additional isotopic effects in soils²¹.

287 Most of the world's biomes are represented; the land uses include grasslands and
288 savannas (34%), forests and woodlands (30%), and annual and perennial crops (36%), from 24
289 countries between latitudes 29° S and 57° N (Extended Data Fig. 1). We selected studies that
290 fulfil the following criteria: the age of change should be known or estimated; the observed depth
291 should be more than 60 cm or reach bedrock; and the difference in the $\delta^{13}\text{C}$ of the vegetation
292 between the reference and the study site should be 5‰ or more in the case of mixed vegetation
293 that include both photosynthetic types. The duration of vegetation change ranged from 4 years
294 to 4,000 years. Authors estimated the dates of change through controlled experiments,
295 enquiries, historical records, or airborne surveys. Changes in isotope signature that occurred
296 more than 1,000 years ago (nine sites) were associated with interacting climate- and man-
297 induced changes in vegetation. In those cases, dates were estimated by the authors from local
298 or regional proxies of palaeovegetation change (for example, pollen/charcoal combined with
299 radiocarbon dating). When the period after vegetation change was expressed by the authors as
300 a range (for changes older than 200 years), we used the mid-value of the range.

301 Mean climatic data were obtained either from data reported in the article ($n = 103$) or,
302 if missing ($n = 9$), from the CRU Group/Oxford/International Water Management Institute
303 (IWMI) 10-minute mean climate grids for global land areas for the period 1961 to 1990 (ref.³¹).
304 We compared grid versus declared climatic data in the database: for annual precipitation, the
305 mean CRU grid/declared ratio is 0.98 ± 0.15 (standard deviation); for MAT, the mean
306 difference between CRU grid and declaration is -0.15 ± 1.1 °C. Topsoil clay content was either

307 obtained from authors' statements or assumed to be the median value of the texture class
308 mentioned. Mean annual aridity indexes, P/PET (annual precipitation/potential
309 evapotranspiration)²³—a better indicator of hydric impact on both net primary production and
310 microbial activity than precipitation alone—were obtained from the Food and Agriculture
311 Organization 10-minute mean climate grids for global land areas for the period 1950 to 2000
312 (ref.²³).

313 **Proportion of new carbon and data pre-processing**

314 For each site, the natural ¹³C-labelling technique uses two plots, which were initially identical,
315 and have been differentiated during the last t years by two types of vegetation that differ in their
316 $\delta^{13}\text{C}$. We use the terms 'reference' ('ref') for the plot at which the vegetation type at the date
317 of sampling is the closest to that of the initial vegetation, and 'studied plot' ('s') for the plot
318 with the new type of vegetation. Most authors described carbon content and isotopic data
319 profiles as successive layers, each one sampled between two depths (z_1, z_2). For each layer ($z_1,$
320 z_2), we define C as the carbon stock in the horizon (in kg m^{-2}); f_{new} as the proportion of new
321 carbon (that is, derived from the new vegetation) (Fig. 1); and C_{new} as the stock of new carbon
322 in the horizon (in kg m^{-2}). C, f_{new} and C_{new} were either obtained from the authors' papers
323 ($n = 30$), or calculated from observed variables as follows. C was calculated from carbon
324 concentration, $[C]$ (in mg g^{-1}), and bulk density, ρ , according to $C = [C] \times \rho \times (z_2 - z_1)$, where
325 ρ was either from the authors' data or (in 41 cases) estimated from $[C]$ according to
326 Alexander's³² equation. f and C_{new} were calculated according to the equations²¹:

$$327 \quad f_{\text{new}} = (\delta\text{soil}_s - \delta\text{soil}_{\text{ref}}) / \Delta\delta\text{veg} \quad (1)$$

$$328 \quad C_{\text{new}} = f_{\text{new}} \times C$$

329 where δsoil_s and $\delta\text{soil}_{\text{ref}}$ are the $\delta^{13}\text{C}$ values of SOC from the study and reference plots; and
330 $\Delta\delta\text{veg}$ is the difference in vegetation $\delta^{13}\text{C}$ between the study and reference plots and was
331 determined from plant or litter samples. The $\delta\text{soil}_{\text{ref}}$ in each horizon was obtained from the
332 reference soil collected at the same depth as the soil of the study plot. In accordance with the
333 limit of resolution of the method, 27 horizons in deep layers had negative f_{new} values; in this
334 case, we considered C_{new} to be 0. The resulting overestimation of average new carbon was
335 negligible. In cases in which the sampling depth differed at the reference and studied plots, we
336 calculated δsoil_s by linear interpolation of the two nearest observed depths. Equation (1)
337 typically accounts for the various ¹³C enrichments that occur during organic carbon decay or
338 historical changes²¹, with the sole criterion that these enrichments are similar in the study and

339 reference soils. Equation (1) neglects the dark fixation of carbon atoms³³ that would have the
340 isotopic composition of atmospheric CO₂.

341 **Depth distribution of new carbon**

342 We calculated depth distributions for the subset of sites whose labelling duration was 200 years
343 or less ($n = 99$; Fig. 3). The mean duration was 35 years. In order to compare similar depth
344 intervals, we calculated the three variables f_{new} , cumulative carbon stock with depth $C(0, z)$ and
345 $C_{\text{new}}(0, z)$ 10-cm increments by linear interpolation of the observed horizons. For each 10-cm
346 depth interval ($z, z + 0.1$ m), we computed the ratio $R = C_{\text{new}}(z, z + 10 \text{ cm})/C_{\text{new}}(0, 100 \text{ cm})$.
347 When bedrock or the R horizon was described, a nil carbon content was attributed to these
348 horizons. When profiles were not described down to a depth of one metre ($n = 31$; most often
349 80 cm), $C(0, 100 \text{ cm})$ was extrapolated from the maximum depth z_{max} using the linear
350 regression $C(0, 100 \text{ cm}) = a \times C(0, z_{\text{max}}) + b$ over the entire data set and similarly for $C_{\text{new}}(0,$
351 $100 \text{ cm})$.

352 The median depth z_{median} of new carbon was calculated for individual profiles as $C_{\text{new}}(0,$
353 $z_{\text{median}}) = C_{\text{new}}(0, 100 \text{ cm})/2$, by linear interpolation in the observed $C_{\text{new}}(0, z)$ function.

354 The variance of the ten ratios $R = C_{\text{new}}(z, z + 10 \text{ cm})/C_{\text{new}}(0, 10 \text{ cm})$ at the ten depths
355 $z = 0, 10, \dots, 90$ cm, the ratio for the whole subsoil $C_{\text{new}}(30, 100 \text{ cm})/C_{\text{new}}(0, 100 \text{ cm})$ and the
356 median depth of new carbon were analysed by multivariate linear regression of time, land use
357 and climatic variables (Extended Data Tables 3–5). Given that the average start date of labelling
358 was 1965, we consider that the regression value of R for time = 50 years stands for carbon
359 incorporated in the time interval 1965–2015. World average values of carbon incorporation in
360 deep soil layers, excluding permafrost areas, were obtained by weighting multivariate linear
361 regression estimates of new carbon (Extended Data Tables 1, 2, 4 and 5) by the biome soil
362 carbon inventories in ref. 5. Multivariate linear regression used the mean value of each of the
363 112 observed profiles, with no weighting for the number of replicates or horizons, leading to
364 less precise but unbiased estimation. When replicated, profile variability is provided in the
365 database in the Supplementary Information. We used bootstrap procedures³⁴ to express
366 confidence on the estimated depth distribution or median age for the globe (Fig. 3 and Extended
367 Data Table 6), or on the depth distribution of ages in tropical grasslands and forests (Fig. 2 and
368 Extended Data Table 3). For that purpose, we drew $N = 100,000$ independent profile bootstrap
369 samples from the observed profiles. For each bootstrap sample, relationships with P/PET,
370 MAT, land use and time were recomputed and used to calculate the values of the variables of

371 interest. Standard deviations were then estimated as the standard deviation of these 100,000
372 values.

373 Statistical analyses were performed using the R packages Boot and Stats version 3.4.3.

374 **Analysis of the inference of vegetation change on the results**

375 The naturally labelled sites experienced varying degrees of perturbation compared with pristine
376 ecosystems. Vegetation change may modify input or decay rates, leading to transient carbon
377 dynamics. To investigate whether these changes themselves affect the depth distribution of new
378 carbon, we tested the dependence on two additional variables that characterize the observed
379 sites: the previous type of vegetation—either crops, grassland or forest, known for 109 sites—
380 and the relative difference in carbon stock between study and reference plots, when known and
381 when the reference resembled the previous vegetation type ($n = 88$ sites). The relative change
382 ΔC_{rel} is calculated as:

$$383 \Delta C_{rel} = [C(0, 100 \text{ cm})_{\text{studied site}} - C(0, 100 \text{ cm})_{\text{reference site}}] / C(0, 100 \text{ cm})_{\text{reference site}}$$

384 ΔC_{rel} is nil on average in the database, that is, it corresponds to the steady state
385 ($\Delta C_{rel} = 0.004 \pm 0.026$, \pm s.e.m.); however, it does vary as a result of changes in inputs or
386 dynamics in different directions. Mean durations of change are independent of previous
387 vegetation in the statistical analysis: 31 years for previous grassland, 37 years for previous
388 crops and 40 years for previous forests (excluding durations of more than 1,000 years, which
389 involve no crop). ΔC_{rel} is not correlated with the duration of the change either.

390 Concerning the depth distribution of new carbon, that is, $R_{30-100} = C_{new}(30 \text{ to}$
391 $100 \text{ cm}) / C_{new}(0 \text{ to } 100 \text{ cm})$, R_{30-100} is not correlated with ΔC_{rel} either in the whole data set
392 ($r^2 = 0.002$; $n = 88$), or within the subsets of crops ($r^2 = 0.01$; $n = 31$), grasslands ($r^2 = 0.02$;
393 $n = 24$) or forests ($r^2 = 0.13$; $n = 33$). We also tested the previous vegetation type as an
394 explanatory variable of R_{30-100} in addition to the other variables of climate, present land use and
395 time (that is, the variables in Extended Data Table 4). The additional variable was not a
396 significant factor (previous forest versus previous crop: $P = 0.88$; previous grassland versus
397 previous crop: $P = 0.52$; previous grass versus previous forest: $P = 0.47$) and did not improve
398 the model.

399 Concerning the proportion of new carbon in either topsoil or subsoil (that is, f_{new}), the
400 previous vegetation type added as an explanatory variable in the statistical models of Extended
401 Data Tables 1 and 2 was not a significant factor either ($P = 0.49$ to 0.99). By contrast, as an
402 additional variable, ΔC_{rel} was highly significant for topsoil ($P < 0.01$) but was not for subsoil

403 ($P = 0.12$). The effect is obvious given that both carbon change and new carbon are first driven
404 by the relative change in inputs. This effect typically explains one of the results, namely the
405 lower proportion of new carbon in cropland topsoils (Extended Data Table 1).

406 Concerning the age distribution in the subset of tropical grasslands and forests (Fig. 2
407 and Extended Data Table 3), the mean value of ΔC_{rel} is very low (0.02 ± 0.03 ; \pm s.e.m.), close
408 to steady state, and ΔC_{rel} does not depend on time, and therefore does not affect the estimated
409 mean age distribution, but does contribute to the random dispersion of results.

410 Finally, we included neither previous vegetation as an explanatory variable in the
411 statistical models of the proportion of new carbon, nor carbon change, because of the covariance
412 of ΔC_{rel} with land use. Furthermore, sites with previous or present croplands may have
413 experienced a complex land-use history involving ancient primary forests and possibly pasture
414 events. Taking all land-use histories into account would become a case-by-case study.

415 On the basis of this analysis of the inference of vegetation changes, we conclude that
416 perturbation did not bias our estimates of the mean depth distribution of new carbon; that is,
417 this depth distribution depends on the present vegetation and conditions, and not on previous
418 vegetation, nor is it affected by non-steady-state conditions, in any systematic direction. The
419 impact of perturbation on the proportion of new carbon in topsoils nevertheless prevented us
420 from integrating our data towards global estimates of the absolute amount of new carbon or
421 global carbon turnover. We thus restricted global integration to the depth distribution and
422 median depth of new carbon.

423 **Data availability**

424 The raw primary data, calculated data and ancillary information analysed and generated here
425 are available in the INRA public repository (<http://dx.doi.org/10.15454/KMNR6R>). No
426 statistical methods were used to predetermine sample size.

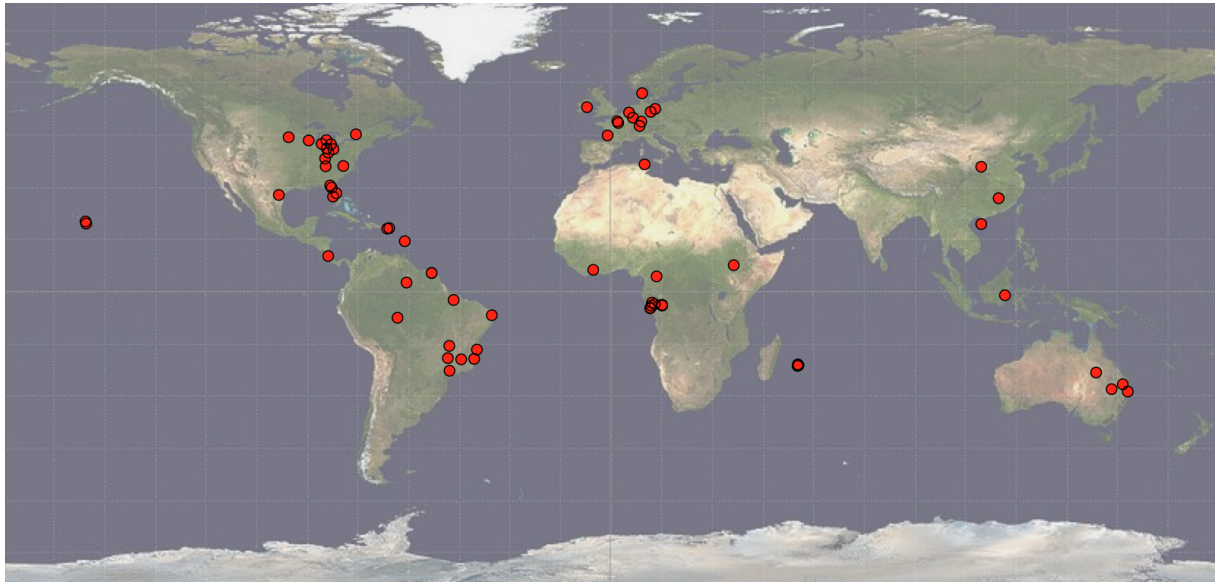
427 31. New, M., Lister, D., Hulme, M. & Makin, I. A high-resolution data set of surface climate over global land
428 areas. *Clim. Res.* 21, 1–25 (2002).

429 32. Alexander, E. B. Bulk densities of California soils in relation to other soil properties. *Soil Sci. Soc. Am. J.*
430 44, 689–692 (1980).

431 33. Šantrůčková, H. et al. Significance of dark CO₂ fixation in arctic soils. *Soil Biol. Biochem.* 119, 11–21
432 (2018).

433 34. Efron, B. & Tibshirani, R. J. *An Introduction to the Bootstrap* (Chapman and Hall, Boca Raton, 1993).

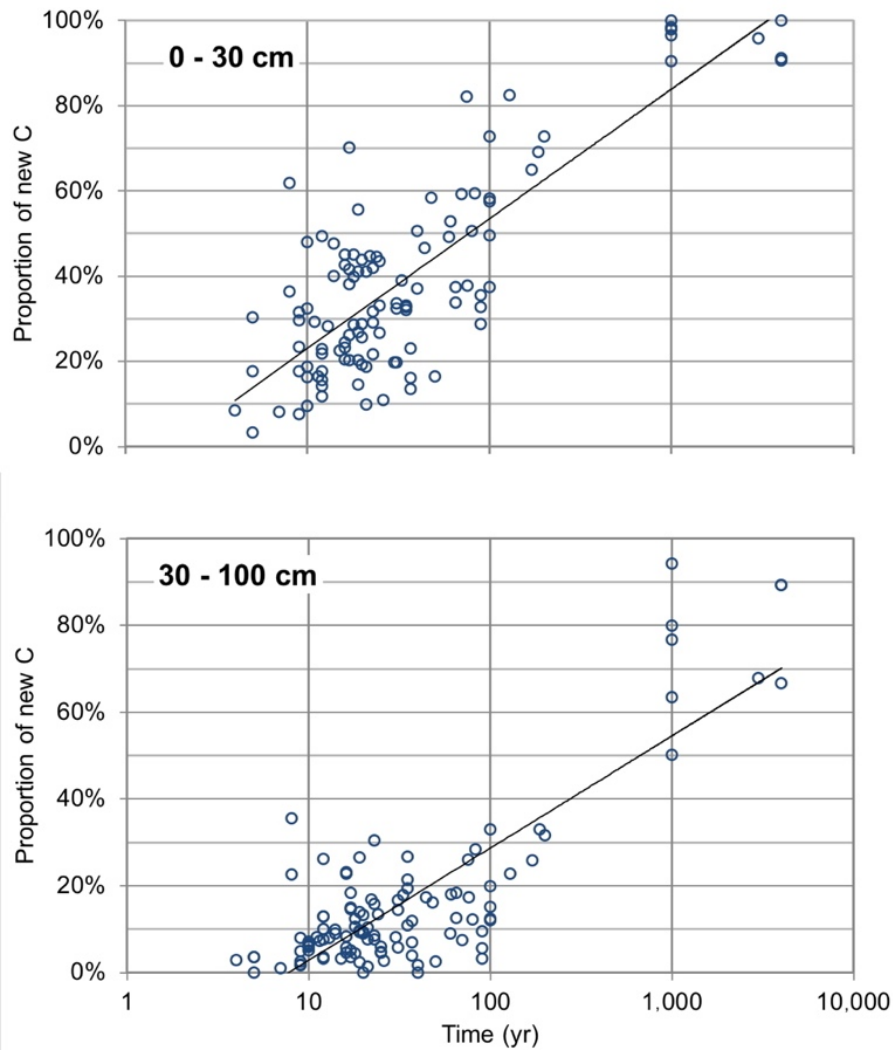
434



436

437 **Extended Data Fig. 1 | Locations of the study sites.** Source of background image: Visible
438 Earth, NASA.

439



440

441 **Extended Data Fig. 2 | Kinetics of new-carbon incorporation for the depth layers 0–30 cm**
 442 **and 30–100 cm.** The respective logarithmic regressions $y = 0.30 \times \log_{10}(x) - 0.07$ for 0–30 cm
 443 and $y = 0.26 \times \log_{10}(x) - 0.23$ for 30–100 cm indicate that the duration required to replace one-
 444 third of the carbon is on average seven times longer in the subsoil than the topsoil.

445

	Coefficient estimate	Standard error	T value	Pr(> T)	
Intercept = Forest	-0.00250	0.0728	-0.034	0.973	
Grassland	-0.0531	0.0405	-1.311	0.193	
Cropland	-0.0951	0.0328	-2.896	0.00472	**
Log10(time)	0.258	0.038	6.865	7.6e-10	***
MAT	0.00595	0.00234	2.540	0.0128	*
P/PET	-0.0441	0.0337	-1.306	0.1954	
Clay	-0.000566	0.000693	-0.816	0.417	

447

448 **Extended Data Table 1 | Proportion of new carbon in topsoil: multivariate linear**
 449 **regression**

450 The dependent variable is the ratio of new carbon (derived from the vegetation after time t) to
 451 total organic carbon in the topsoil layer. The explanatory variables are land use (grassland or
 452 cropland), $\log_{10}(t)$ (in years), mean annual temperature (MAT, in °C), ratio of annual
 453 precipitation to evapotranspiration (P/PET), and topsoil clay content (as a percentage). The
 454 reference land use (intercept) is forest. T is the value of Student's statistics; $\text{Pr}(>|T|)$ is the
 455 probability value of the Student's test.

456 * $P < 0.05$; ** $P < 0.01$; *** $P < 0.001$.

457 Residual standard error, 0.1249 on 92 degrees of freedom; multiple R^2 , 0.4781; adjusted R^2 ,
 458 0.444; F -statistic, 14.04 on 6 and 92 degrees of freedom; P -value, 2.768×10^{-11} .

459

	Coefficient estimate	Standard error	T value	Pr(> T)	
Intercept = Forest	0.0205	0.0433	0.474	0.637	
Grassland	-0.0136	0.0241	-0.564	0.574	
Cropland	0.0024	0.0195	0.121	0.904	
Log10(time)	0.0849	0.0223	3.806	0.00025	***
MAT	0.00216	0.00139	1.551	0.124	
P/PET	-0.0516	0.0201	-2.570	0.0118	*
Clay	0.000018	0.000412	0.045	0.965	

460

461 **Extended Data Table 2 | Proportion of new carbon in subsoil: multivariate linear**
462 **regression**

463 The dependent variable is the ratio of new carbon (derived from the vegetation after time t) to
464 total organic carbon in the subsoil layer. See Extended Data Table 1 for further definitions.
465 Residual standard error, 0.07424 on 92 degrees of freedom multiple R^2 , 0.2561; adjusted R^2 ,
466 0.2076; F -statistic, 5.279 on 6 and 92 degrees of freedom; P -value, 0.0001028

467

Depth	a_1	k_1 (yr ⁻¹)	a_2	k_2 (yr ⁻¹)	$a_1 + a_2$	Standard deviation of residuals
0 cm	0.614 (0.47, 0.75)	0.21 (0.11, 2.8)	0.34 (0.2, 0.49)	0.0073 (0.0024, 0.0158)	0.95 (0.92, 1.0)	0.18
10 cm	0.287 (0.19, 0.40)	0.15 (0.08, 0.5)	0.67 (0.56, 0.77)	0.0059 (0.0028, 0.0083)	0.96 (0.94, 1.0)	0.11
20 cm	0.108 (0.05, 0.19)	0.23 (0.09, 1.5)	0.85 (0.78, 0.92)	0.0047 (0.0025, 0.0072)	0.95 (0.92, 1.0)	0.09
30 cm	0.074 (0.02, 0.13)	0.24 (0.13, 1.5)	0.86 (0.8, 0.93)	0.0035 (0.0020, 0.0064)	0.93 (0.88, 1.0)	0.10
40 cm	0.070 (0.03, 0.13)	0.23 (0.09, 1.0)	0.83 (0.74, 0.93)	0.0026 (0.0014, 0.0041)	0.90 (0.83, 1.0)	0.10
50 cm	0.066 (0.04, 0.11)	0.21 (0.10, 0.5)	0.80 (0.70, 0.95)	0.0020 (0.0010, 0.0030)	0.87 (0.79, 1.0)	0.09
60 cm	0.065 (0.03, 0.11)	0.20 (0.10, 0.4)	0.75 (0.65, 0.89)	0.0018 (0.0008, 0.0028)	0.82 (0.73, 0.94)	0.10
70 cm	0.052 (0.02, 0.09)	0.22 (0.13, 0.5)	0.71 (0.62, 0.88)	0.0016 (0.0007, 0.0024)	0.76 (0.67, 0.95)	0.10
80 cm	0.044 (0.01, 0.08)	0.25 (0.15, 3.2)	0.65 (0.54, 0.92)	0.0016 (0.0005, 0.0024)	0.70 (0.60, 0.93)	0.11
90 cm	0.042 (0.01, 0.08)	0.25 (0.14, 3.5)	0.60 (0.46, 0.99)	0.0016 (0.0003, 0.0025)	0.64 (0.51, 1.0)	0.11
100 cm	0.048 (0.01, 0.08)	0.25 (0.14, 3.3)	0.55 (0.44, 0.99)	0.0014 (0.0002, 0.0025)	0.60 (0.48, 1.0)	0.11

468

469

470

471

472

473

474

475

476

477

478

479

480

Extended Data Table 3 | Age distribution of carbon over 55 tropical grassland and forest soil profiles

These data were used to generate Fig. 2. At each depth, the proportion f_{new} of carbon aged less than t was fitted by a nonlinear regression of time t using the equation $f_{\text{new}} = a_1.[1 - \exp(-k_1 \times t)] + a_2.[1 - \exp(-k_2 \times t)]$. Such bi-exponential functions³⁰ describe carbon age distribution, with carbon divided into three age classes, a_1 being the proportion of ‘young’ carbon, a_2 the proportion of ‘old’ carbon, and $(1 - a_1 - a_2)$ the proportion of carbon with an infinite age. $1/k_1$ and $1/k_2$ are the mean ages of young and old carbon, respectively. Numbers in parentheses denote the 95% confidence intervals of the estimated parameters. The median environmental conditions of the soil set are: MAT = 23.6 °C; annual precipitation = 2,100 mm; P/PET (ref.²³) = 1.44 and topsoil clay content = 37%.

	Coefficient estimate	Standard error	T value	Pr(> T)	
Intercept = Forest	0.193	0.049	3.979	0.00014	***
Grassland	0.0218	0.03499	0.624	0.534	
Cropland	0.105	0.029	3.646	0.00044	***
Time (yr)	0.000369	0.000320	1.155	0.251	
MAT (°C)	0.00381	0.00206	1.848	0.0677	
P/PET	-0.0996	0.0297	-3.354	0.00116	**
Clay (%)	0.000638	0.000608	1.049	0.297	

481

482 **Extended Data Table 4 | Depth incorporation of new carbon in subsoil: multivariate linear**
483 **regression**

484 The dependent variable is the ratio of the amount of new carbon (derived from the vegetation
485 after time t , in kg m^{-2}) in the subsoil layer to the amount of new carbon in the entire top metre—
486 that is, $R_{30-100} = C_{\text{new}}(30 \text{ to } 100 \text{ cm})/C_{\text{new}}(0 \text{ to } 100 \text{ cm})$. See Extended Data Table 1 for further
487 definitions. Note the dependence on time: the maximum value of the coefficient at the 95%
488 confidence level (estimate + 2 s.e.m.) is 0.001 yr^{-1} . Residual standard error, 0.11 on 92 degrees
489 of freedom; multiple R^2 , 0.2387; adjusted R^2 , 0.1891; F -statistic, 4.808 on 6 and 92 degrees of
490 freedom; P -value, 0.0002618

491

	Coefficient estimate	Standard error	T value	Pr(> T)	
Intercept = Forest	11.3	2.183	5.174	1.31e-06	***
Grassland	3.93	1.463	2.689	0.00849	**
Cropland	8.77	1.28	6.842	8.18e-10	***
Time (yr)	0.0201	0.0137	1.466	0.146	
MAT (°C)	0.183	0.089	2.045	0.0437	*
P/PET	-5.11	1.32	-3.871	0.000202	***

492

493

Extended Data Table 5 | Median depth of new carbon: multiple linear regression.

494

The dependent variable is the median depth (in cm) of the amount of new carbon (carbon derived from the vegetation after time t , in kg m^{-2}) of each profile. See Extended Data Table 1 for further definitions. Residual standard error, 4.963 on 93 degrees of freedom; multiple R^2 , 0.3985; adjusted R^2 , 0.3662; F -statistic, 12.32 on 5 and 93 degrees of freedom; P -value: 3.551×10^{-9} .

495

496

497

498

499

500

	Observed Forests	Observed Grasslands	Observed Croplands	Global estimate
0-10 cm	0.538 (0.048)	0.511 (0.071)	0.321 (0.032)	0.521 (0.046)
10-20 cm	0.174 (0.026)	0.188 (0.021)	0.237 (0.019)	0.189 (0.020)
20-30 cm	0.084 (0.016)	0.092 (0.020)	0.159 (0.017)	0.098 (0.017)
30-40 cm	0.052 (0.012)	0.056 (0.012)	0.091 (0.013)	0.056 (0.009)
40-50 cm	0.037 (0.007)	0.045 (0.011)	0.065 (0.010)	0.040 (0.008)
50-60 cm	0.032 (0.007)	0.028 (0.010)	0.037 (0.007)	0.030 (0.008)
60-70 cm	0.024 (0.006)	0.022 (0.010)	0.026 (0.005)	0.022 (0.006)
70-80 cm	0.023 (0.007)	0.022 (0.009)	0.023 (0.005)	0.021 (0.006)
80-90 cm	0.014 (0.006)	0.020 (0.007)	0.019 (0.004)	0.013 (0.007)
90-100 cm	0.013 (0.005)	0.018 (0.007)	0.017 (0.004)	0.011 (0.008)

501

502 **Extended Data Table 6 | Depth distribution of carbon transferred from atmosphere to**
503 **SOM in 1965–2015**

504 These data were used to generate Fig. 3. The amount of new carbon transferred from the
505 atmosphere to SOM in 1965 to 2015 (< 50 yr carbon) in each 10-cm layer is expressed as a
506 proportion of the total new carbon < 50 yr in the first metre. The data shown are mean values
507 for observed forests, grasslands and croplands, and global estimates; the numbers in parentheses
508 are the 95% confidence intervals on the mean or estimate.

509

510